

## Dating fluvial terraces with $^{10}\text{Be}$ and $^{26}\text{Al}$ profiles: application to the Wind River, Wyoming

Gregory S. Hancock <sup>a,\*</sup>, Robert S. Anderson <sup>a</sup>, Oliver A. Chadwick <sup>b</sup>,  
Robert C. Finkel <sup>c</sup>

<sup>a</sup> *Department of Earth Sciences and Institute of Tectonics, University of California, Santa Cruz, CA 95064, USA*

<sup>b</sup> *Department of Geography, University of California, Santa Barbara, CA 93106, USA*

<sup>c</sup> *Center for Accelerator Mass Spectrometry, Lawrence Livermore National Laboratory, Livermore, CA 94550, USA*

Received 11 July 1997; revised 13 February 1998; accepted 11 May 1998

### Abstract

Fluvial strath terraces provide a record of river incision and the timing of climatic perturbations to the fluvial system. Dating depositional surfaces like terraces that are older than the range of  $^{14}\text{C}$ , however, is difficult. We employ a cosmogenic radionuclide (CRN) profile technique that addresses a major problem of CRN dating on such surfaces: nuclide inheritance. By measuring  $^{10}\text{Be}$  and  $^{26}\text{Al}$  profiles, we constrain the exposure age and the mean CRN inheritance for the deposit. The CRN profile also yields a self-check on the assumptions underlying the method. We report our attempts to date terraces along the Wind River, WY. Like many sequences of western North American fluvial terraces, these are inferred to reflect oscillation between glacial and interglacial conditions in the headwaters. Previous dating of some of these terraces and the associated terraces and glacial deposits makes this a unique location to compare dating methods. Dates from five sites along the Bull Lake-glacial correlative terrace (WR-3) are  $\sim 118$ – $125$  ka, which agrees with dates on Bull Lake-age moraines and independent age estimates on the terrace, and is consistent with the model of terrace–glacial relationship. CRN inheritance is significant and highly variable, requiring it be considered despite the additional sampling complexity. Assuming all inheritance in WR-3 deposits arises during exhumation in the headwaters, we obtain minimum mean rates of exhumation of  $\sim 13$ – $130$  m/My for the source rocks. Alternatively, assuming the CRNs are inherited during clast transport, the time of fluvial transport from source to terrace is  $> \sim 10$  ka; it increases downstream and is lower for sand than cobbles. The CRN ages for older terraces (WR-7 =  $\sim 300$  ka and WR-15 =  $\sim 510$  ka) are lower by  $\sim 50\%$  than previous estimates based on tephrochronology; the most plausible explanation is eolian deflation of a once thicker loess cover on the terrace surfaces. Mean thicknesses of loess of  $\sim 0.5$ – $1.5$  m are required to reconcile these concentrations of CRN with the previous estimates of age. Difficulty in dating the older terraces emphasizes that geologic caution, independent estimates of age, and multiple sample sites should still be part of dating depositional surfaces with CRNs, even when employing the inheritance-correction technique. © 1999 Elsevier Science B.V. All rights reserved.

*Keywords:* fluvial terraces; inheritance-correction technique; cosmogenic radionuclide

\* Corresponding author. Present address: Department of Geology, College of William and Mary, Williamsburg, VA 23187, USA. E-mail: gshanc@facstaff.wm.edu

## 1. Introduction

Fluvial strath terraces mark the position of a downcutting river through time, and provide a record of river incision and the timing of perturbations to the fluvial system. Strath terraces are abandoned river channels and floodplains above the active channel, formed as a river migrates laterally during periods of relatively constant river elevation. This migration widens the valley floor, and bevels a bedrock platform that is covered by thin alluvium. This platform becomes a terrace upon abandonment when climatic and/or tectonic changes lead to river incision.

Many river systems in the Rocky Mountain and Colorado Plateau region of western North America retain a fluvial strath terrace record of discontinuous downcutting into bedrock throughout the late Quaternary. Absolute and relative ages have been obtained on many of these terraces by tephrochronology, stratigraphic correlation, and radiometric dating. Many terrace sequences appear to record the fluvial response to local oscillations between glacial and interglacial conditions, with formation of the straths and deposition of the capping alluvium occurring during periods of maximum headwater glaciation (e.g., Ritter, 1967; Howard, 1970; Sinnock, 1981; Reheis et al., 1991). Strath formation may reflect a transition to braided stream conditions initiated by increased sediment supply and hydrologic changes associated with glacial periods. Incision may occur during interglacials, or periods of transition from interglacial to glacial conditions (Sinnock, 1981). If indeed these terraces are linked to glacial episodes, they may provide a record of glacial conditions that is better preserved and more complete in time than the moraine records in the headwaters. In addition, acceleration of the rates of incision of rivers during the Quaternary has been noted in many locations (e.g., Patton et al., 1991; Reheis et al., 1991; Repka et al., 1997; Chadwick et al., 1997) suggesting a response of the rates of incision of rivers to some regional forcing.

In this paper we present our work on dating a sequence of fluvial terraces along the Wind River, WY. Because depositional features like fluvial terraces are difficult to date numerically, we have developed a dating technique, modified from Ander-

son et al. (1996), that employs cosmogenic radionuclide (CRN) profiles. We first discuss the Wind River basin field area and the preserved terrace sequence, and review the existing glacial chronology established for this region. We then present the details of our CRN profile technique; our technique and the concerns leading to its development are relevant for dating depositional features of any type. We then present the results, and conclude with a discussion addressing the following questions: (1) is the CRN profile strategy that we outline for dating these features worth the effort?; (2) how do our terrace ages compare with previous estimates, and what do they imply about terrace formation?; (3) what is the incision history of the Wind River suggested by our ages?, and (4) what is the magnitude of CRN 'inheritance' in this system, and what does it imply about sediment exhumation and transport histories?

## 2. The Wind River basin

### 2.1. *Geology and climate*

The Wind River basin, located in northwestern Wyoming, is delineated by the Wind River Range, Owl Creek Mountains, and Granite Mountains to the southwest, north, and southeast, respectively, and the volcanic Absaroka Range to the northwest (Fig. 1). The Wind River rises along the continental divide in the northern Wind and southern Absaroka ranges, and flows southeastward along the front of the Wind River Range front for ~200 km (Fig. 1). At Riverton, the Wind River turns north and cuts the Wind River Canyon through the Owl Creek Mountains, where the river gradient steepens in response to encountering resistant Precambrian and Paleozoic rocks (Fig. 2). Once through the Wind River Canyon, it becomes the Bighorn River. The bedrock underlying the river in the Wind River Basin is mainly siltstones and mudstones of basin-filling Eocene Wind River Formation; some short reaches cross northeast-dipping and more resistant Mesozoic rocks (Fig. 2). Along most of its course above the Wind River Canyon, the Wind River flows on alluvial fill, not directly on bedrock. The basins in this region (e.g., Wind, Bighorn, Green) were primarily deposi-

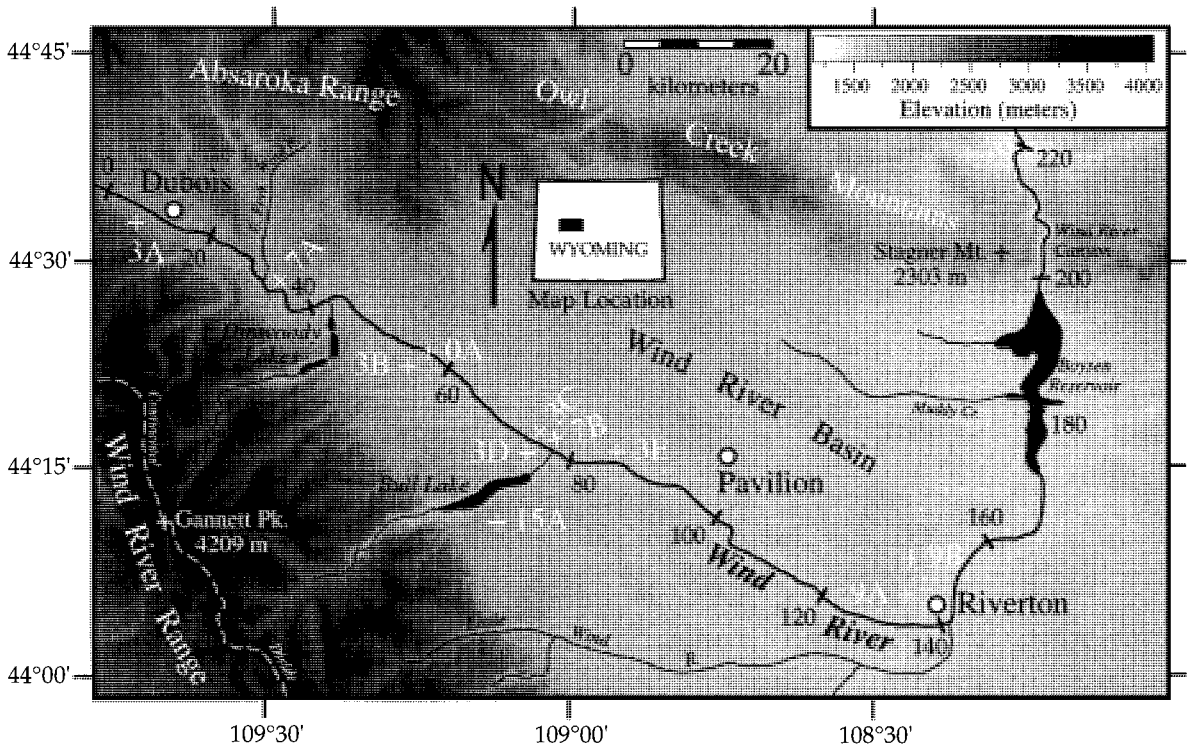


Fig. 1. Map of sample site locations in the Wind River region and river kilometers.

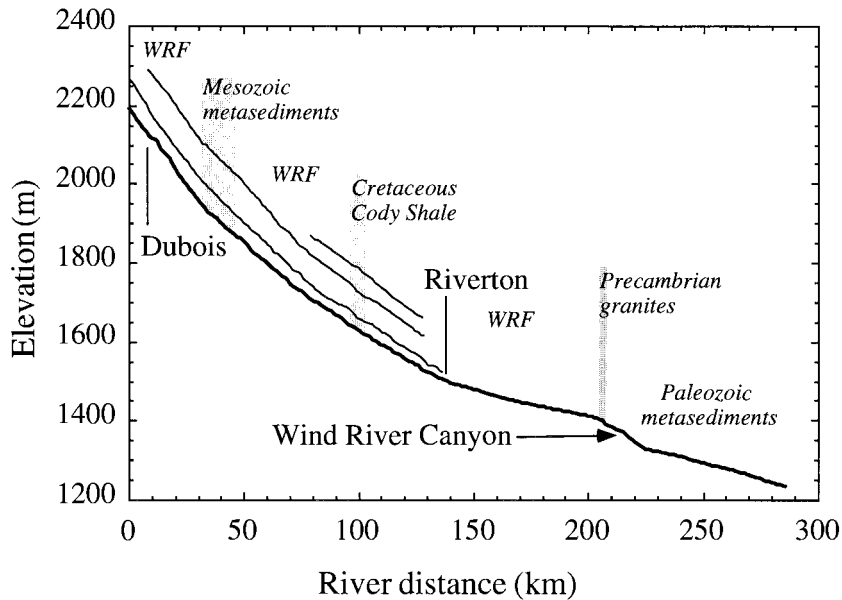


Fig. 2. Profile of modern Wind River with underlying geology (WRF refers to the Eocene Wind River Formation). Geology from Morris et al. (1959). The river steepens in the Wind River Canyon, where it responds to encountering the more resistant Precambrian and Paleozoic rocks of the Owl Creek Mountains. These rocks act as a local base level for the Wind River upstream of the canyon.

tional through the early Tertiary; regional uplift beginning in the Pliocene has led to extraction of much of the basin fill sediments (Love, 1979).

Climate in this region is frigid and arid to semi-arid. Mean annual precipitation (period of record: 1951–1980) is 21.8 cm at Dubois, 19.8 cm at Pavilion, and 20.6 cm at Riverton (see Fig. 1 for locations); at higher elevations in the Wind River Range, total precipitation reaches many times that in the basin. Mean annual temperature at Riverton is  $\sim 6.0^{\circ}\text{C}$ . Peak discharges in the annual Wind River hydrograph are typically associated with spring snow melt, occurring in late May through late June. Recorded annual peak discharges range from 16–55  $\text{m}^3/\text{s}$  at Dubois (1946–1992) and 51–377  $\text{m}^3/\text{s}$  at Riverton (1906–1994). Drainage area along the study reach is  $\sim 1260 \text{ km}^2$  at Dubois,  $\sim 5980 \text{ km}^2$  at Riverton, and  $\sim 19,940 \text{ km}^2$  at the Wind River Canyon.

## 2.2. Glacial chronology of the Wind River region

A well-established glacial chronology exists for the last several 100 thousand years before present (ka) for the Wind River region. Blackwelder (1915) first proposed the Pinedale, Bull Lake, and Buffalo glaciations in the Wind River Range, and correlated

them with the late and early Wisconsin and Illinoian glaciations, respectively, of mid-continental North America. The Pinedale and Bull Lake deposits have since become the type locales for correlative glacial deposits in the Rocky Mountain region. On the basis of obsidian hydration ages, Pierce et al. (1976) assigned ages of 25–35 ka for the Pinedale and 130–155 ka for the Bull Lake glacial deposits in Yellowstone. Cosmogenic radionuclide dating techniques have provided a second set of numeric age estimates for moraines in drainages within the Wind River Range. Gosse et al. (1995) suggest the Pinedale glacial maximum was reached by  $\sim 22 \text{ ka}$  at Fremont Lake near Pinedale; similarly, at Bull Lake, the CRN dating ( $^{36}\text{Cl}$  and  $^{10}\text{Be}$ ) of the Pinedale-age moraine complex yields ages from 16 to 23 ka (Phillips et al., 1997; note that ages given here are in CRN years, which equal calendar years only if rates of production are correct, which is a matter of ongoing debate; see Clark et al., 1995; Nishiizumi et al., 1996). Dates on four Bull Lake-age moraine complexes at Bull Lake (Fig. 1), yield CRN ( $^{36}\text{Cl}$  and  $^{10}\text{Be}$ ) ages of  $> 130 \text{ ka}$ , 120 to 128 ka, 121 to 105 ka, and 100 to 110 ka (Phillips et al., 1997). Whereas evidence exists for glacial conditions during isotope stage 4 elsewhere in western North America (e.g., Richmond and Fullerton, 1986; Phillips et al., 1990;

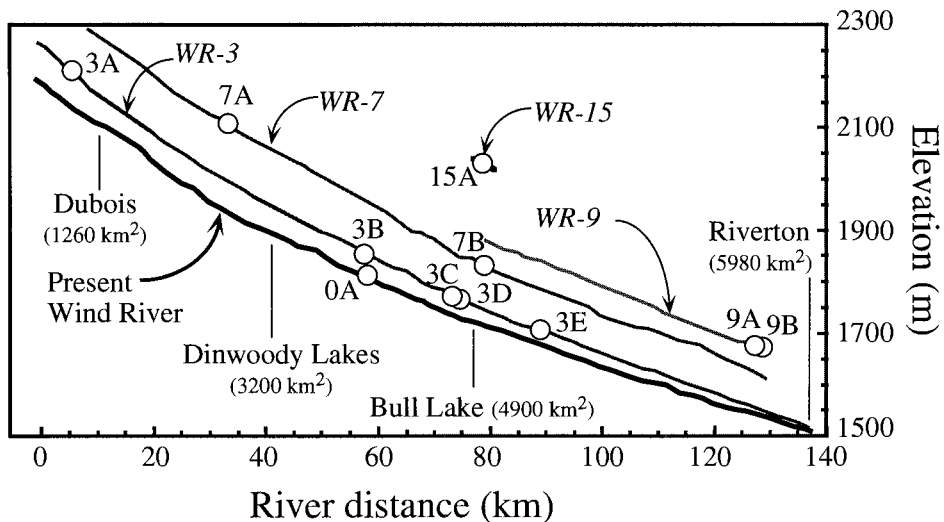


Fig. 3. Profiles of modern Wind River and terraces WR-3, WR-7, WR-9, and WR-15, after Chadwick et al. (1997). Sample sites are shown as open circles with site numbers; Wind River drainage area above selected locations also shown. Terrace elevations above the modern river decrease in the downstream direction, and suggest a long-term reduction in river slope over this reach.

Forman et al., 1993; Repka et al., 1997), little conclusive evidence exists for a glaciation during this time in the Wind River Range (Hall and Shroba, 1993; Hall and Shroba, 1995).

Whereas moraines of at least one older glacial advance, named the Sacagawea Ridge, are mapped in the Wind River Basin (Blackwelder, 1915; Richmond and Murphy, 1965), numeric ages are not well



Fig. 4. View of modern Wind River and several terraces, looking upstream and south from terrace WR-7 (~ 170 m above river level, sample site 7A). Fluvial gravels are exposed on the surface of the terrace. Terrace WR-3 is above the road on right, ~ 55 m above river level. Road is constructed on terrace WR-1.

constrained for this advance. Sacagawea Ridge moraines at Dinwoody Lakes yield limiting  $^{36}\text{Cl}$  and

$^{10}\text{Be}$  model ages of  $> 232$  ka (Phillips et al., 1997), and  $> 125$ – $297$  ka (Evenson et al., 1994; J. Gosse,



Fig. 5. View of terrace subsurface at sample site 9B showing the imbricated fluvial gravels, thin sand lenses (near middle and bottom of deposit), and capping silt layer (upper  $\sim 45$  cm) that are typical of the deposits of the Wind River terraces. Numerous quartzite clasts (or quartz sands) are collected at several depths in such exposures; equal masses of quartzite are extracted from each clast and combined into one sample. We analyzed samples from several depths to obtain the mean CRN profile in a deposit, which allow an estimation of deposit age and mean inheritance.

pers. comm.). A fluvial terrace along the Wind River (WR-7) that may be correlative with the Sacagawea Ridge outwash has been dated at  $\sim 660$  ka, because it contains a deposit of volcanic ash identified as the Lava Creek B (Jaworowski, 1992; Chadwick et al., 1997).

### 2.3. The Wind River terraces

Fifteen separate strath terrace levels (numbered WR-1 to WR-15 from youngest to oldest) have been mapped along the Wind River above Riverton (Fig. 2, Chadwick et al., 1997; Figs. 3 and 4). Initial work by Blackwelder (1915) identified three terraces in the Wind River basin, calling them the Black Rock (WR-15), Circle (Bull Lake-age WR-3) and Lenore (Pinedale-age WR-1) terraces. Morris et al. (1959) identified 13 chronologically distinct terraces, including terraces preserved along tributaries (e.g., Muddy Creek) draining the unglaciated Owl Creek Mountains (Fig. 1). Morris et al. (1959) suggested uplift or tilting of the basin, enlargement of the drainage area through capture, climatic change, or base level change as possible mechanisms to drive the development of terraces. They inferred that streams forming the straths had higher discharges than the modern counterparts. Chadwick et al. (1997) and Phillips et al. (1997) have more recently mapped and identified 15 terrace levels, and have dated several with in situ  $^{36}\text{Cl}$  and  $^{10}\text{Be}$  (WR-1  $\sim 16$  to 23 ka and WR-3  $\sim 100$  to 125 ka) and tephrochronology (WR-7 =  $\sim 660$  ka). The ages on these terraces were used to calculate rates of incision, which were then extrapolated to estimate ages for the remaining terrace levels. This pre-existing chronology provides a rare opportunity to compare numeric ages obtained by several methods to the estimates of CRN age we present in this paper.

The Wind River terraces are straths thinly mantled by primarily braided stream deposits (Fig. 5). On the most extensive terrace (WR-3), total thickness of alluvial deposits varies from  $\sim 25$  m at Dubois to a few meters near Riverton (Chadwick et al., 1997). The terrace gravels are predominantly Absaroka Range volcanics, Wind River Range granites and Mesozoic sedimentary rocks, and quartzite cobbles. These quartzite cobbles are likely extracted from conglomerates within the Middle Eocene Ay-

cross Formation, and possibly the Paleocene Pinyon Conglomerate. The Aycross outcrops along the base of the Absaroka Range to the north of the Wind River, and could provide quartzite cobbles to the river downstream of the Dubois area (Fig. 1). Mapped outcrops of the Pinyon lie just across the divide between the Wind River and Snake River basins north of the Wind River Range, but is not identified in locations which could be contributing to the river between Dubois and Riverton (Fig. 1). The terrace deposits are typically clast supported, with either an openwork or sand matrix, and are composed of 50–75% gravel-sized material. Grain sizes range from fine sands to boulders ( $< 50$  cm). Discrete layers of up to  $\sim 1$  m separated by unconformities are seen in several exposures. Gravels are imbricated, confirming that they remain in the original depositional position. Thin ( $< 20$  cm), cross-bedded sand lenses occur locally, but no significant silt or clay lenses were observed within the gravel deposits. An eolian/fluvial silt layer with thicknesses of a few tens of cm to  $\sim 2$  m usually overlies the fluvial cobbles and sands on all terraces (example in Fig. 5). Fluvial cobbles ( $< 10$  cm) are scattered on the surface of the eolian/fluvial silt layer; some similarly-sized floating clasts are occur within the silt layer. These clasts have likely been upfrozen from the fluvial deposits below the silt layer.

## 3. Cosmogenic radionuclide profile dating

### 3.1. Theory and dating technique

We utilize the CRNs  $^{10}\text{Be}$  ( $t_{1/2} = 1.50$  My) and  $^{26}\text{Al}$  ( $t_{1/2} = 0.705$  My). CRNs are produced in situ in material at the surface primarily by bombardment of target nuclei by secondary cosmic ray particles (Bierman, 1994; Cerling and Craig, 1994). The production rate,  $P$ , of CRNs in solid material decreases with depth,  $z$ :

$$P(z) = P_0 \cdot e^{-(z/z^*)} \quad (1)$$

where  $P_0$  is the rate of production at the surface and the decay length scale is  $z^* = \Lambda/\rho$ , where  $\rho$  is the density of the overlying material, and  $\Lambda$  is the absorption mean free path. The values for  $\Lambda$  used here are  $\sim 150$  g/cm $^2$  (Brown et al., 1992).

In depositional settings like fluvial terraces, the total concentration of a CRN in a sample from the deposit (e.g., a cobble) has two components: (1) CRNs accumulated prior to deposition (the ‘inheritance’,  $N_{in}$ ), and (2) CRNs accumulated following deposition,  $N_{dep}$  (Anderson et al., 1996). Combining these, the concentration,  $N$ , of a CRN in a sample is a function of the deposit age,  $t$ , and depth,  $z$ :

$$N(z, t) = \frac{P(z)}{\lambda} \cdot (1 - e^{-\lambda t}) + N_{in} \cdot e^{-\lambda t} \quad (2)$$

where  $P(z)$  is the rate of production (Eq. (1)), and  $\lambda$  is the decay constant ( $\ln 2/t_{1/2}$ ). The first term in Eq. (2) represents the growth of an exponential CRN profile following deposition, whereas the second term represents the decay of the inherited component (Fig. 6). This formulation assumes no surface erosion or burial and no correction for muon-produced isotopes. If the age of the surface being dated is much shorter than the half-life of the isotopes, then we can simplify this equation to:

$$N(z, t) = N_{surf}(t)e^{-z/z^*} + N_{in} \quad (3)$$

where  $N_{surf} = P_0 t$ , the CRN concentration at the surface of the deposit.

The inheritance,  $N_{in}$ , includes CRNs acquired during exhumation from the source ( $N_{exh}$ ) and during transport from the source to the deposit ( $N_{trans}$ ). In this setting, CRNs accumulated in a clast before it was incorporated into the source are negligible, because the youngest source conglomerates were deposited in the Eocene,  $> \sim 15^{10}\text{Be}$  half-lives ago. Deposit materials (e.g., cobbles) are likely to have experienced a wide variety of transport and exhumation histories, giving  $N_{in}$  a stochastic nature and making depositional surfaces potentially difficult to date with CRNs (Fig. 6; Anderson et al., 1996). This variability in  $N_{in}$  primarily arises from differences in grain size, source area, lithology, and transport distance of materials from the source. Because of the unknown contribution of  $N_{in}$  to the total CRN concentration, CRN exposure ages obtained from any single clast in a deposit must be considered, at best, a maximum.

We correct for inheritance by using a clast amalgamation and multiple sample depth technique improved from that described in Anderson et al. (1996) because we use CRN profiles rather than sample

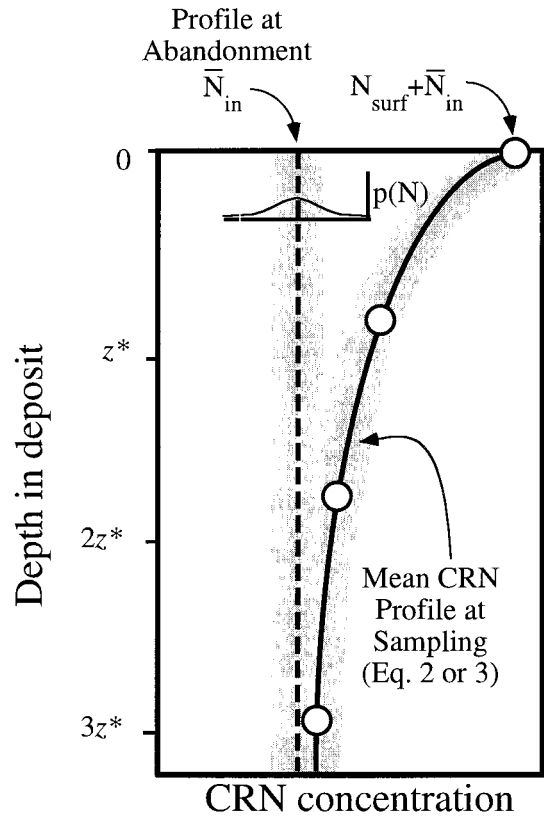


Fig. 6. Schematic of two mean CRN profiles in a deposit—one upon abandonment (dashed line), one at some time,  $t$ , later when deposit is sampled (solid curve). Our dating technique assumes that, whereas inheritance is likely highly variable among individual clasts (illustrated by the gray speckled region around the curves), the mean inheritance,  $\bar{N}_{in}$ , is equal throughout the deposit. If this is the case, then the mean CRN profile at deposition should be equal throughout the deposit, as shown. The CRN profile grows exponentially with time,  $t$ , again with some variation around the mean resulting from the variable inheritance. By determining the mean concentration of CRN at several depths with amalgamated samples (open circles), we can estimate the mean CRN profile (solid line) for the deposit. We then use linear regression of Eq. (2) (Eq. (3) if decay is not important) to determine the age and mean inheritance for the deposit.

pairs. At a discrete depth in a deposit, we collect numerous quartzite clasts or quartz sand grains. We collect and isolate quartz for our CRN analysis because (1) it provides appropriate and abundant target nuclei for  $^{10}\text{Be}$  (oxygen) and  $^{26}\text{Al}$  (silicon); (2) it is resistant to chemical weathering and is resistant to contamination by meteoric CRNs; (3) it is abundant in the terrace deposits; and (4) rates of production



for these CRN in quartz have been calibrated (e.g., Nishiizumi et al., 1996). Equal masses of quartz are taken from each clast and are combined into one sample. The CRN downconcentration measured in this amalgamated sample includes: (1) the mean inheritance,  $\bar{N}_{in}$ , for the clasts going into the amalgamated sample; and (2)  $N_{dep}$ , which should be equal for all clasts because they are collected from a fixed depth (i.e., nearly equal  $P(z)$  for each). Assuming we have amalgamated enough clasts to obtain  $\bar{N}_{in}$  for the sampling depth, this concentration is the mean CRN concentration at that sampling depth,  $\bar{N}(z, t)$ .

By repeating this process at several depths, we obtain points on the mean CRN profile in a deposit (Fig. 6). Assuming that (1) the mean inheritance,  $\bar{N}_{in}$ , is not a function of depth within the deposit; (2) the material has not been significantly displaced post-depositionally (e.g., by frost heave); and (3) deposition was rapid relative to the age of the deposit, then the CRN concentrations should fall on an exponential profile defined by Eq. (2) (or Eq. (3) if decay is not significant). We use simple linear regression to obtain the age and the inheritance from the measured CRN profiles. This method is an advance over the two-sample method outlined in Anderson et al. (1996), because the full CRN profile

provides a more robust test of the assumptions above; if significantly violated, an exponentially-decaying CRN profile would not be obtained. The age obtained with this method corresponds to the time since deposition of the terrace, assuming that the rate of production of CRNs in the terrace deposits has not been significantly altered by factors such as significant erosion of and/or deposition on the surface, burial by snow cover, or growth of significant vegetation on the terrace surface. In the Wind River system, the later two are not likely to be significant, given the arid, frigid, and windy climate found in the Wind River basin. The possibility for loess cover is discussed below as a possibility on several terrace surfaces.

### 3.2. Sample collection and analysis

Samples were collected from one site on the modern floodplain (WR-0), and from 10 sites on four terrace levels (5 WR-3, 2 WR-7, 2 WR-9, and 1 WR-15) along the Wind River between Dubois and Riverton, WY (~125 river km, Figs. 1 and 3; Table 1). These are the most spatially extensive terraces (WR-3, WR-7, and WR-9) and the oldest terrace (WR-15) along the study reach. We collected modern river gravels to determine (1) if inheritance is

Table 1  
Sites of Wind River terrace samples

Terrace <sup>a</sup>	Assigned age (ka) (Chadwick et al., in press)	Site number	River km	Height above WR at Bull Lake (m)	Latitude (degrees N)	Site Selevation (m)	Production correction factor <sup>b</sup>	Silt cover thickness (cm)
Modern	0	0A	57	0	43.4	1801	4.21	NA
WR-3	103–126 <sup>c</sup>	3A	5	65	43.5	2194	5.56	30
		3B	57	50	43.3	1847	4.35	35
		3C	73	40	43.3	1775	4.13	40
		3D	75	40	43.3	1768	4.10	30
		3E	89	20	43.2	1707	3.92	30
WR-7	~ 660 <sup>d</sup>	7A	33	135	43.5	2121	5.29	NA
		7B	79	120	43.3	1829	4.29	NA
WR-9	950 <sup>e</sup>	9A	127	115	43.0	1640	3.72	60
		9B	129	115	43.1	1640	3.73	46
WR-15	1740 <sup>e</sup>	15A	79	290	43.1	1999	4.82	43

<sup>a</sup>Terrace numbers follow nomenclature of Chadwick et al. (1994).

<sup>b</sup>Calculated as in Lal (1991).

<sup>c</sup>CRN (<sup>36</sup>Cl) age.

<sup>d</sup>Tephrochronology age (Lava Creek B ash).

<sup>e</sup>Extrapolation of WR-7 incision rate.

significant and (2) how many clasts would be needed to constrain the mean inheritance. Whereas conditions in the modern river may not reflect conditions during terrace deposition, these samples should still provide at least an indication of the magnitude and variability of inheritance. We collected samples where subsurface access was available, and where the terrace surfaces were not obviously degraded by anthropogenic and/or geomorphic processes. We estimated the elevation and latitude of the site from 1:24,000 USGS topographic quadrangle maps (Table 1). Correction factors for horizontal shielding, calculated following Nishiizumi et al. (1993), were very near 1.0 at all sites, which indicates that the topographic shielding effect on rates of production is negligible.

We estimated the density of terrace materials to obtain values for the decay length scale,  $z^*$  (Eq. (1)). Samples from the silt layer collected at three locations yielded a mean bulk density of  $1.5 \pm 0.1$  g/cm<sup>3</sup>. To constrain the density of gravel deposits, we took photographs (e.g., Fig. 5) of cross-sections cut through the deposits, from which we estimate that the deposits are composed of 50–75% clasts larger than coarse sand by volume. Assuming a clast density of 2.7 g/cm<sup>3</sup>, and a 30% porosity and grain density of 2.7 g/cm<sup>3</sup> for the interstitial sand, the deposits have a density of roughly 2.5 g/cm<sup>3</sup>, with an assumed error of  $\pm 0.1$  g/cm<sup>3</sup>. This value is comparable to field measurements on alluvial gravels elsewhere (Vincent and Chadwick, 1994). With these densities, values for  $z^*$  range from  $58 \pm 4$  to  $96 \pm 6$  cm in the Wind River terrace deposits, depending on the thickness of the silt layer and depth of the sample.

To obtain the rates of surface production at each sampling location, we use the calibrated sea-level, high latitude value of 5.80 atoms <sup>10</sup>Be/g quartz-year (Nishiizumi et al., 1996), corrected for latitude, altitude, and topographic shielding. The correction factors are given in Table 1, and we assume an error of  $\pm 10\%$  in the rates of production provided by Nishiizumi et al. (1996). The debate regarding CRN the magnitude and error of the rates of production continues (e.g., Clark et al., 1995), and, therefore, our estimates of terrace ages will likely be subject to revision as these are refined. The rate of production of <sup>26</sup>Al is taken to be 6.04 times the <sup>10</sup>Be production

rate (Nishiizumi et al., 1989). We assume that the geomagnetic latitude over the exposure lifetime of the terraces averages out to the current geographic latitude; this likely introduces negligible error given the ages ( $\geq 100$  ka) of the dated terraces. We do not attempt to correct the rate of CRN production for variations in the intensity of the magnetic field. All of our dates are given in CRN years and allow straightforward correction for future refinements in the histories of rates of production.

At each site, we typically selected several depths, including the terrace surface, from which to collect numerous quartzite clasts with long dimensions of  $\sim 5$ –20 cm. At sites 3B and 9B, we also took quartz-rich sand from several depths. The physical processing of quartz-rich sand is simpler than cobbles. The large number of individual grains in a sample provide a better estimate of the mean concentration of CRN. Material was collected over a narrow depth interval ( $\pm 5$  cm) and horizontal extent ( $< 2$  m). Collection over a restricted depth range is required because the rate of CRN production is a function of depth (Eq. (1)). For a depth range of  $\pm 5$  cm and typical values for  $z^*$ , the range of  $P(z)$  is  $\sim \pm 5\%$ . Each cobble in a suite is crushed, and an equal mass of quartz is taken from each and combined into one sample, which is then pulverized and sieved. Quartz sands are sieved only. The 2.5  $\phi$  to 1.0  $\phi$  (0.177 to 0.50 mm) fraction is retained after sieving. If a significant non-quartz fraction remains, the material is passed through a magnetic separator, density separation, and a 50% *o*-phosphoric acid leach to dissolve non-quartz silicates (Talvitie, 1951; D. Grainger, pers. comm., 1996).

The amalgamated quartz samples are then purified for analysis using the method of Kohl and Nishiizumi (1992). We add  $\sim 1$  g of stable 1000 ppm <sup>9</sup>Be and <sup>27</sup>Al carrier solution to the samples. Stable <sup>9</sup>Be and <sup>27</sup>Al concentrations are determined by inductively coupled plasma mass spectrometry (ICP-MS) at UCSC, and the <sup>10</sup>Be/<sup>9</sup>Be and <sup>26</sup>Al/<sup>27</sup>Al ratios in the samples are determined by accelerator mass spectroscopy (AMS; Elmore and Phillips, 1987; Finkel and Suter, 1993) at the Lawrence Livermore National Laboratories (LLNL) Center for Accelerator Mass Spectrometry. Ratios are normalized to LLNL standards for <sup>10</sup>Be and <sup>26</sup>Al. The ratios, measured in process blanks prepared in parallel with the field

samples, are subtracted from the results; typical corrections are  $\leq 1\%$ .

## 4. Analytical results and interpretation

### 4.1. Analytical results and errors

The analytical results are presented in Table 2. The calculated errors in the concentration of CRN include propagation of uncertainties in the AMS analyses ( $\sim \pm 5\%$ ), stable isotope carrier concentration ( $\sim \pm 2\%$ ), and ICP-MS analyses ( $\sim \pm 2\%$ ). Age errors include uncertainties in sea level, high latitude rate of production ( $\pm 10\%$ ); deposit density ( $\sim \pm 5\%$ ); latitude and altitude corrections ( $\pm 10\%$ ); and absorption mean free path ( $\sim \pm 5\%$ ), except where noted. We neglect errors in the rate of production introduced by changes in the intensity of the magnetic field because of current uncertainty in the calibrations of the rate of production; however, if the correction for the intensity of the magnetic field were applied to the WR-3 sample sites, it would result in a reduction of estimated ages by  $\sim 10\%$  (Clark et al., 1995). To allow direct comparison between sites, all concentrations of CRN used in the figures and discussion are normalized by dividing the actual abundance (Table 2) by the correction factor for latitude and altitude (Table 1).

### 4.2. Inheritance in modern Wind River (WR-0) samples

We analyzed five quartz samples composed of nine clasts each collected from the modern Wind River (Site 0A, Fig. 1). The five samples yielded concentrations ranging over three orders of magnitude (Table 2). Interpreted as model ages for CRN, the  $^{10}\text{Be}$  and  $^{26}\text{Al}$  concentrations yield ranges of  $< 3.6$  ka to  $202 \pm 42$  ka CRN years and  $0.655 \pm 0.21$  ka to  $122 \pm 19$  ka CRN years, respectively. These samples suggest that inheritance is a substantial CRN contributor in terraces younger than several 100 ka, and is highly variable. If single clasts were collected from the surfaces of the terraces, it is likely that ages would vary even more widely.

We would like to estimate the number of clasts required to constrain the mean inheritance, within a

specified standard deviation. To do so, we use a maximum likelihood, least squares method which assumes a Gaussian distribution of the inheritance in the clast population (J. Revenaugh, pers. comm., 1997). By assuming that the variance of clast concentration of CRN within each amalgamated sample is equal to the variance of all the samples,  $\tilde{\sigma}^2$ , and given  $m$  is the number of amalgamated clasts in each sample (9 in this case), we can estimate the variance of the entire population of clasts as  $\tilde{\sigma}_p^2 = m\tilde{\sigma}^2$ . The number of clasts,  $c$ , required to obtain a specified standard deviation,  $\tilde{\sigma}_{in}$ , around the mean inheritance is  $c = \tilde{\sigma}_p^2 / \tilde{\sigma}_{in}^2$ . Ignoring samples 082295-2B (analytical results for  $^{10}\text{Be}$  below detection) and 082295-2D (apparent outlier), the measured value for  $\bar{N}_{in}$  at site 0A is 0.091 atoms  $^{10}\text{Be}/\mu\text{g}$  quartz and 0.47 atoms  $^{26}\text{Al}/\mu\text{g}$  quartz, and the standard deviation of the clast population, is 0.12 atoms  $^{10}\text{Be}/\mu\text{g}$  quartz and 0.59 atoms  $^{26}\text{Al}/\mu\text{g}$  quartz (Table 3). The corresponds to mean inherited ages of  $\sim 16$  ka for  $^{10}\text{Be}$  and  $\sim 14$  ka for  $^{26}\text{Al}$ . The variance implies that  $\sim 31$  clasts must be amalgamated in a sample to obtain an estimate of  $\bar{N}_{in}$  with a  $\tilde{\sigma}_{in} = \pm 20\%$ .

### 4.3. Fluvial strath terrace CRN profiles and ages

#### 4.3.1. Terrace WR-3

The measured CRN profiles for WR-3 terrace sites 3A, 3C, and 3E are shown in Fig. 7. The profiles display an exponential decay with depth (Eqs. (1) and (2)), ignoring the surface samples from sites 3C and 3E. The surface clasts at sites 3C and 3E have likely been exposed since deposition to mean rates of production of CRN below that of the surface rate,  $P_0$ . Because of this possibility, we do not use the surface clasts in the profiles from 3C and 3E to estimate ages. Estimated  $^{10}\text{Be}$  model ages obtained from the profiles range from  $102 \pm 10$  ka to  $137 \pm 22$  ka, and  $^{26}\text{Al}$  ages range from  $108 \pm 11$  to  $174 \pm 69$  ka (excluding 3D), with a mean CRN age of  $118 \pm 33$  ka and  $125 \pm 37$  ka for  $^{10}\text{Be}$  and  $^{26}\text{Al}$ , respectively (Table 3). The corresponding values of for each site, shown as dashed ( $^{10}\text{Be}$ ) and solid ( $^{26}\text{Al}$ ) lines in Fig. 7, are also given in Table 3; inheritance is 7–20% of the predicted post-depositional concentration of CRN at the surface,  $N_{\text{surf}}$ .

The mean WR-3  $^{10}\text{Be}$  age ( $\sim 118$  ka) is consistent with terrace genesis during deposition of the two

Table 2  
Analytical results of Wind River terrace samples

Sample site and sample number	Sample depth (m)	$z^*$ (cm)	# clasts	Quartz extracted (g)	$^{27}\text{Al}$ in quartz (ppm)	Concentration (atoms/ $\mu\text{g}$ quartz)		$^{10}\text{Be}/^{26}\text{Al}$ ratio	Uncorrected model ages (ka)	
						$^{10}\text{Be}$	$^{26}\text{Al}$		$^{10}\text{Be}$	$^{26}\text{Al}$
<i>Site 0A</i>										
082295-2A	0.00 ± 0.00	NA	9	19.9885	197	0.614 ± 0.033	3.37 ± 0.19	5.49 ± 0.42	25.3 ± 5.1	23.1 ± 3.5
082295-2B	0.00 ± 0.00	NA	9	19.9610	153	< 0.0879	0.0975 ± 0.027	NA	< 3.61	0.661 ± 0.21
082295-2C	0.00 ± 0.00	NA	9	19.9900	128	0.104 ± 0.020	0.528 ± 0.054	5.06 ± 1.11	4.28 ± 1.3	3.59 ± 0.63
082295-2D	0.00 ± 0.00	NA	9	20.3283	185	4.71 ± 0.15	17.1 ± 0.71	3.64 ± 0.19	202 ± 42	123 ± 19
082295-2E	0.00 ± 0.00	NA	9	20.1307	169	0.437 ± 0.029	2.10 ± 0.16	4.79 ± 0.48	18.0 ± 3.7	14.3 ± 2.3
<i>Site 3A</i>										
082095-4	0.00 ± 0.00	NA	30	19.9974	173	3.49 ± 0.12	23.3 ± 1.0	6.68 ± 0.38	111 ± 22	127 ± 20
082095-3	0.45 ± 0.05	83	23	5.6793	96	2.12 ± 0.083	13.3 ± 0.73	6.28 ± 0.42	116 ± 23	120 ± 19
082095-2	1.10 ± 0.10	71	19	9.1130	115	0.933 ± 0.048	5.78 ± 0.26	6.19 ± 0.43	141 ± 29	134 ± 19
<i>Site 3B</i>										
060295-8	1.26 ± 0.01	71	27	19.9922	522	1.00 ± 0.047	5.51 ± 0.27	5.50 ± 0.37	246 ± 53	207 ± 31
060295-6 <sup>a</sup>	1.93 ± 0.05	69	NA	30.0860	77	0.266 ± 0.020	1.52 ± 0.064	5.69 ± 0.49	182 ± 41	145 ± 19
060295-5 <sup>a</sup>	2.25 ± 0.08	68	NA	30.1093	70	0.202 ± 0.016	0.846 ± 0.045	4.18 ± 0.40	232 ± 53	128 ± 17
060295-7	2.30 ± 0.15	68	21	8.3972	108	0.544 ± 0.033	3.17 ± 0.30	5.82 ± 0.65	752 ± 200	657 ± 130
<i>Site 3C</i>										
060295-12	0.00 ± 0.00	NA	30	20.0078	236	2.30 ± 0.11	13.4 ± 0.57	5.83 ± 0.36	98.4 ± 20	97.5 ± 15
060295-13	0.49 ± 0.08	89	26	13.0406	191	1.90 ± 0.064	10.5 ± 0.56	5.54 ± 0.35	141 ± 29	129 ± 20
060295-15	1.02 ± 0.11	74	18	19.9958	417	0.600 ± 0.10	5.57 ± 0.26	9.28 ± 1.67	101 ± 29	147 ± 22
060295-10	1.75 ± 0.25	70	19	19.9995	239	0.603 ± 0.10	3.14 ± 0.14	5.20 ± 0.93	327 ± 10	248 ± 35
<i>Site 3D</i>										
092894-3	0.00 ± 0.00	NA	29	20.0074	215	2.12 ± 0.056	13.2 ± 0.49	6.21 ± 0.29	90.9 ± 18	96.0 ± 15
092894-1,2	1.50 ± 0.10	69	28	20.0213	211	0.798 ± 0.038	3.83 ± 0.17	4.80 ± 0.32	316 ± 69	224 ± 32
<i>Site 3E</i>										
082395-1	0.00 ± 0.00	NA	30	7.2467	166	1.94 ± 0.075	11.0 ± 0.48	5.66 ± 0.33	87.0 ± 17	83.2 ± 13
082295-3	0.55 ± 0.05	79	30	10.3378	116	1.97 ± 0.071	10.3 ± 0.44	5.24 ± 0.29	181 ± 37	155 ± 24
082295-4	0.95 ± 0.05	72	30	19.9838	341	1.63 ± 0.064	8.50 ± 0.43	5.22 ± 0.33	286 ± 61	237 ± 37
082295-5	1.30 ± 0.10	70	25	6.2034	95	0.950 ± 0.062	4.78 ± 0.29	5.04 ± 0.45	286 ± 65	218 ± 33
<i>Site 7A</i>										
082295-1A	0.00 ± 0.00	NA	10	15.2196	184	9.00 ± 0.28	48.0 ± 2.2	5.34 ± 0.30	315 ± 68	300 ± 52
082295-1B	0.00 ± 0.00	NA	10	15.0923	194	8.10 ± 0.25	NA	NA	282 ± 60	NA
<i>Site 7B</i>										
082295-3A	0.00 ± 0.00	NA	20	15.0238	210	3.63 ± 0.18	19.6 ± 0.75	5.40 ± 0.34	151 ± 31	140 ± 22
082295-3B	0.00 ± 0.00	NA	20	14.9951	242	4.53 ± 0.13	25.2 ± 1.0	5.56 ± 0.27	190 ± 39	183 ± 29
<i>Site 9A</i>										
082395-3A	1.75 ± 0.05	73	21	20.2321	152	5.18 ± 0.16	18.7 ± 0.51	3.60 ± 0.15	NA	NA
082395-3B	1.75 ± 0.05	73	21	20.0733	169	4.65 ± 0.13	23.6 ± 0.73	5.07 ± 0.22	NA	NA
082395-4A	2.35 ± 0.05	70	21	20.0627	201	2.78 ± 0.088	13.5 ± 0.52	4.85 ± 0.24	NA	NA
082395-4B	2.35 ± 0.05	70	21	19.3740	212	2.39 ± 0.092	12.6 ± 0.42	5.28 ± 0.27	NA	NA
<i>Site 9B</i>										
060395-1	0.00 ± 0.01	NA	30	20.0221	796	4.73 ± 0.16	22.5 ± 0.90	4.75 ± 0.25	232 ± 48	190 ± 30
060395-5 <sup>a</sup>	1.16 ± 0.00	74	NA	20.4238	111	0.716 ± 0.036	3.85 ± 0.17	5.37 ± 0.36	164 ± 34	135 ± 19
BR-1 <sup>a</sup>	1.13 ± 0.05	74	NA	20.1370	96	0.671 ± 0.043	3.90 ± 0.24	5.81 ± 0.51	146 ± 31	130 ± 19

Table 2 (continued)

Sample site and sample number	Sample depth (m)	$z^*$ (cm)	# clasts	Quartz extracted (g)	$^{27}\text{Al}$ in quartz (ppm)	Concentration (atoms/ $\mu\text{g}$ quartz)		$^{10}\text{Be}/^{26}\text{Al}$ ratio	Uncorrected model ages (ka)	
						$^{10}\text{Be}$	$^{26}\text{Al}$		$^{10}\text{Be}$	$^{26}\text{Al}$
<i>Site 9B</i>										
060395-4B	1.23 $\pm$ 0.00	74	20	18.2525	145	1.05 $\pm$ 0.046	5.14 $\pm$ 0.21	4.90 $\pm$ 0.29	273 $\pm$ 59	204 $\pm$ 30
BR-2 <sup>a</sup>	1.62 $\pm$ 0.05	71	NA	20.1500	90	0.503 $\pm$ 0.030	2.36 $\pm$ 0.13	4.70 $\pm$ 0.39	240 $\pm$ 53	163 $\pm$ 23
BR-3 <sup>a</sup>	1.99 $\pm$ 0.04	70	NA	20.8600	96	0.370 $\pm$ 0.023	1.50 $\pm$ 0.10	4.06 $\pm$ 0.38	319 $\pm$ 73	178 $\pm$ 26
060395-3 <sup>a</sup>	2.00 $\pm$ 0.10	70	NA	15.5281	91	0.446 $\pm$ 0.045	1.88 $\pm$ 0.12	4.22 $\pm$ 0.50	396 $\pm$ 100	232 $\pm$ 34
060395-2	2.11 $\pm$ 0.00	69	25	20.0128	372	0.932 $\pm$ 0.038	3.68 $\pm$ 0.15	3.95 $\pm$ 0.23	1150 $\pm$ 350	636 $\pm$ 110
<i>Site 15A</i>										
082895-4AB	0.00 $\pm$ 0.00	NA	20	11.1183	207	14.8 $\pm$ 0.57	68.1 $\pm$ 2.5	4.61 $\pm$ 0.24	604 $\pm$ 146	514 $\pm$ 97
082895-4CD	0.00 $\pm$ 0.00	NA	20	13.2058	138	12.5 $\pm$ 0.49	63.3 $\pm$ 2.7	5.07 $\pm$ 0.29	500 $\pm$ 120	468 $\pm$ 87
082895-3A	1.16 $\pm$ 0.06	73	8	16.3345	129	3.50 $\pm$ 0.14	17.4 $\pm$ 0.62	4.98 $\pm$ 0.27	709 $\pm$ 180	589 $\pm$ 100
082895-3B	1.16 $\pm$ 0.06	73	8	13.7538	121	3.68 $\pm$ 0.15	23.1 $\pm$ 1.9	6.28 $\pm$ 0.57	753 $\pm$ 190	890 $\pm$ 210
082895-2A	1.60 $\pm$ 0.10	71	8	14.7648	258	2.14 $\pm$ 0.092	9.89 $\pm$ 0.42	4.62 $\pm$ 0.28	894 $\pm$ 240	647 $\pm$ 120
082895-2B	1.60 $\pm$ 0.10	71	8	12.6222	180	2.17 $\pm$ 0.096	11.5 $\pm$ 0.97	5.30 $\pm$ 0.51	907 $\pm$ 250	805 $\pm$ 180

<sup>a</sup>Sample amalgamated from quartz sand.

youngest Bull Lake-age glacial advances dated by Phillips et al. (1997). This is consistent with a model of terrace formation during periods of maximum glacial extent in the adjacent mountain ranges. The

age places WR-3 formation in late isotope stage 6 or early stage 5 (Fig. 8; Imbrie et al., 1984), but the errors associated with the technique do not allow any further discrimination than this. Our  $^{10}\text{Be}$  dates (102

Table 3

Estimated CRN surface concentration and CRN inheritance and terrace ages corrected for inheritance

Terrace number	Site	Normalized $N_{\text{surf}}$ (a/ $\mu\text{g}$ quartz)		Normalized $N_{\text{in}}$ (a/ $\mu\text{g}$ quartz) <sup>a</sup>		Inheritance-corrected model age (ka)	
		$^{10}\text{Be}$	$^{26}\text{Al}$	$^{10}\text{Be}$	$^{26}\text{Al}$	$^{10}\text{Be}$	$^{26}\text{Al}$
WR-3 <sup>b</sup>	0A	0 $\pm$ 0	0 $\pm$ 0	0.091	0.47	0 $\pm$ 0	0 $\pm$ 0
	3A	0.58 $\pm$ 0.003	4.0 $\pm$ 0.17	0.043 $\pm$ 0.002	0.15 $\pm$ 0.12	102 $\pm$ 10	121 $\pm$ 13
	3B (c)	0.77 $\pm$ 0.077	4.5 $\pm$ 0.45	0.099 $\pm$ 0.026	0.40 $\pm$ 0.28	137 $\pm$ 22	108 $\pm$ 44
	3B (s)	0.62 $\pm$ 0.062	3.6 $\pm$ 0.362	0.024 $\pm$ 0.009	0.08 $\pm$ 0.23	109 $\pm$ 39	174 $\pm$ 69
	3C	0.67 $\pm$ 0.24	3.6 $\pm$ 0.07	0.045 $\pm$ 0.091	0.45 $\pm$ 0.03	119 $\pm$ 45	108 $\pm$ 11
	3D	> 0.36 $\pm$ 0.036	> 2.2 $\pm$ 0.216	< 0.153 $\pm$ 0.057	< 1.05 $\pm$ 0.34	> 64 $\pm$ 8.7	> 78 $\pm$ 13
	3E	0.70 $\pm$ 0.28	3.8 $\pm$ 1.5	0.170 $\pm$ 0.096	0.84 $\pm$ 0.53	124 $\pm$ 53	115 $\pm$ 46
	WR-3 Mean	0.67 $\pm$ 0.13	3.90 $\pm$ 0.51			118 $\pm$ 33	125 $\pm$ 37
WR-7 <sup>d</sup>	7A	1.62 $\pm$ 0.05	9.1 $\pm$ 0.142	NA	NA	298 $\pm$ 34	300 $\pm$ 52
	7B	0.77 $\pm$ 0.036	5.2 $\pm$ 0.205	NA	NA	137 $\pm$ 16	161 $\pm$ 17
WR-9 <sup>c</sup>	9A	11.5 $\pm$ 1.145	35.2 $\pm$ 3.52	0.288 $\pm$ 0.163	1.91 $\pm$ 0.38	5200 $\pm$ 4600	NA
	9B (c)	1.13 $\pm$ 0.113	5.45 $\pm$ 0.545	0.150 $\pm$ 0.08	0.65 $\pm$ 0.30	204 $\pm$ 24	169 $\pm$ 13
	9B (s)	0.48 $\pm$ 0.048	3.65 $\pm$ 0.365	0.086 $\pm$ 0.01	0.27 $\pm$ 0.04	85 $\pm$ 12	110 $\pm$ 9.0
WR-15 <sup>c</sup>	15A	2.64 $\pm$ 0.264	12.29 $\pm$ 1.229	0.230 $\pm$ 0.13	1.90 $\pm$ 0.57	511 $\pm$ 37	431 $\pm$ 29

c,s denote cobble or sand sample, respectively.

<sup>a</sup>Inheritance concentration errors do not take into account the number of clasts amalgamated, and, therefore, errors are likely larger than reported.

<sup>b</sup> $N_{\text{surf}}$  and  $N_{\text{in}}$  determined by linear regression of Eq. (3).

<sup>c</sup>Age and  $N_{\text{in}}$  determined by linear regression of Eq. (2); age errors do not include rate of production and analytical errors.

<sup>d</sup>Ages are not corrected for inheritance.

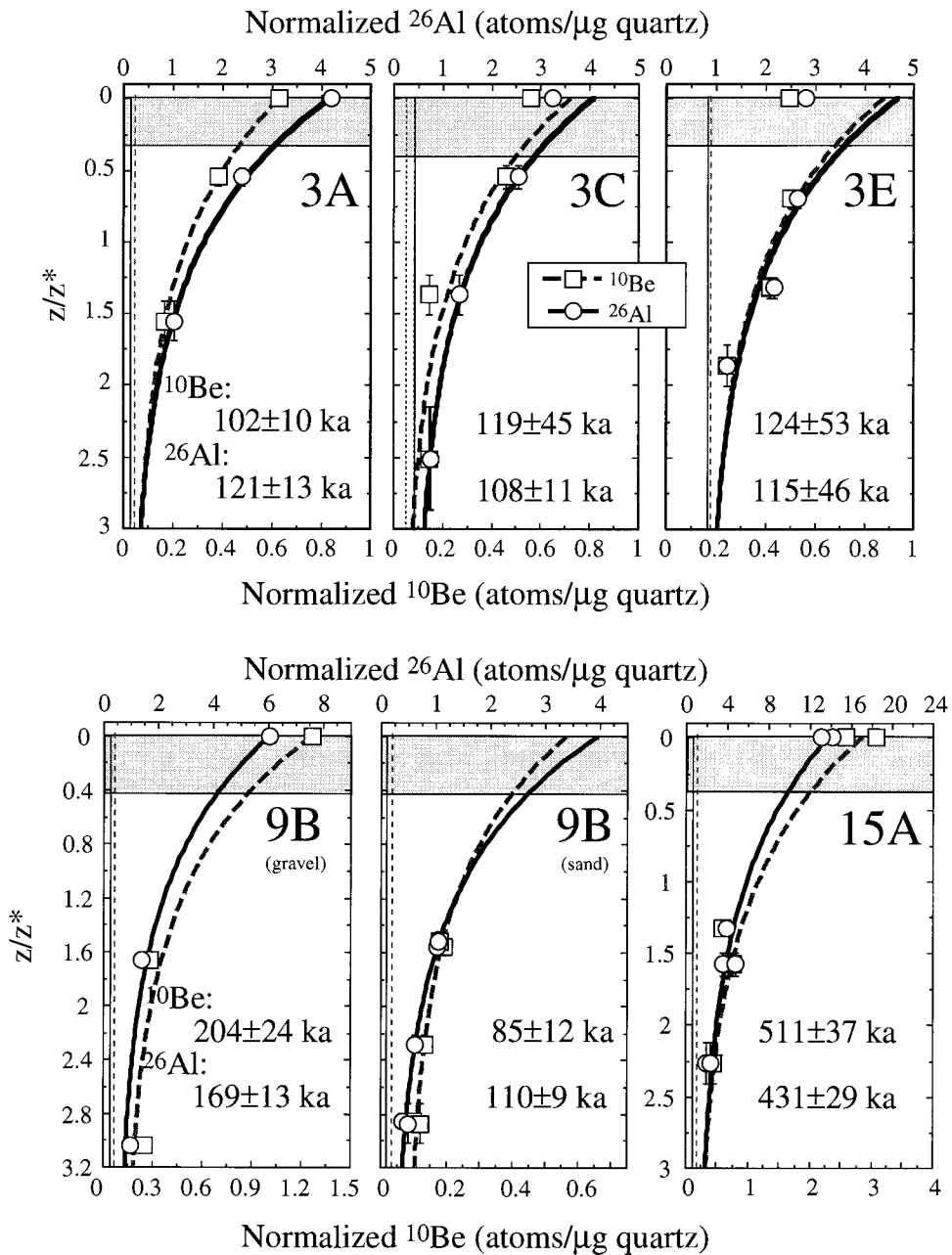


Fig. 7. Normalized CRN sample concentrations vs. normalized depth in the terrace ( $^{10}\text{Be}$  shown with boxes,  $^{26}\text{Al}$  with squares) and best fitting CRN profiles determined by linear regression for sites 3A, 3C, 3E, 9B, and 15A. Error bars are plotted for the concentration of CRN, and the depth range over which each sample is collected. Concentrations of CRN ( $x$ -axis) are normalized to sea-level, high latitude. Normalized depth ( $y$ -axis) is obtained by dividing the depth of the sample by the production length scale,  $z^*$ . The gray boxes show the thickness of the silt layer, below which lie intact gravels. Exposure ages and mean inheritance ( $^{10}\text{Be}$  dashed line,  $^{26}\text{Al}$  solid) calculated from profile fits are shown. We use Nishiizumi et al. (1996) rates of CRN production to determine ages. The concentrations of CRN in surface clasts for sites 3C and 3E are lower than predicted by extrapolating the exponential profile to the surface; these surface samples are not used in the profile fits. The anomalous concentrations may reflect exposure to a mean rate of CRN production less than the current surface rate, perhaps because of turbation or deflation of the silt layer.

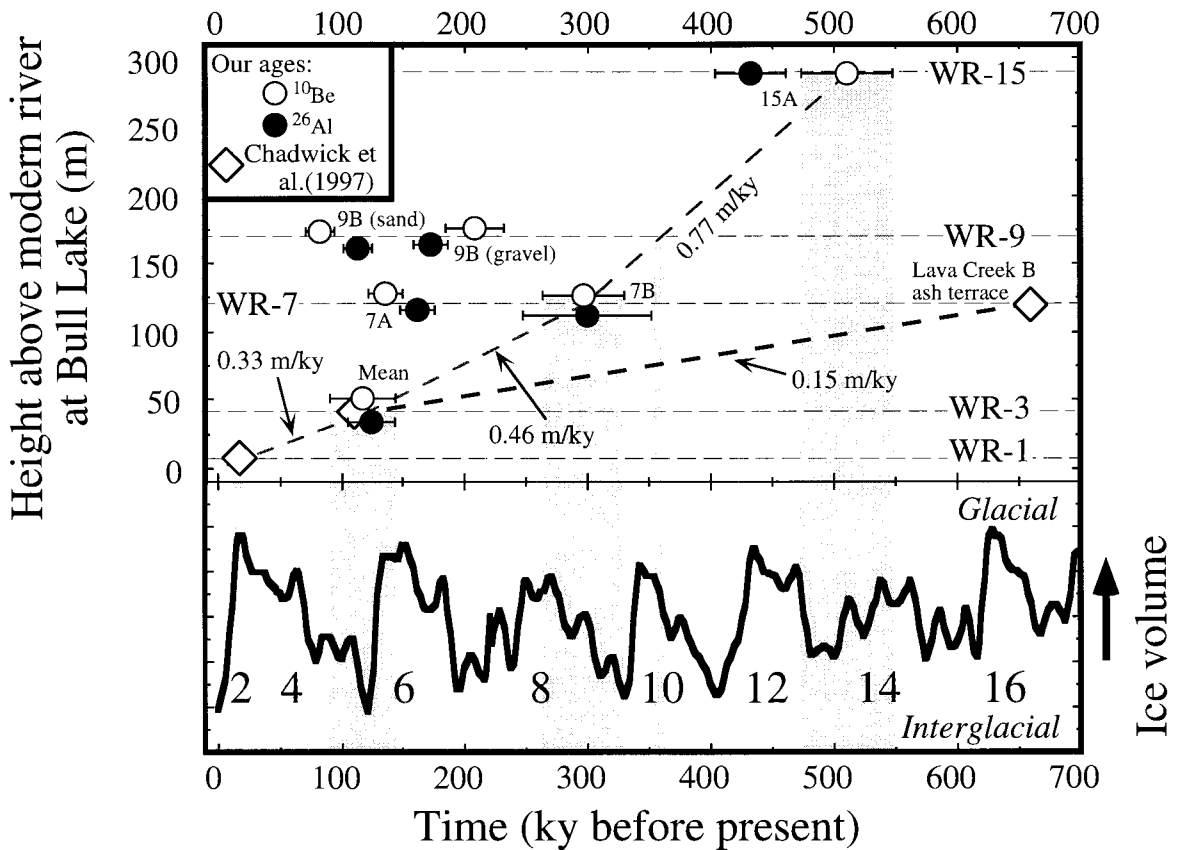


Fig. 8. Upper graph shows height above modern river at Bull Lake vs. estimated terrace ages from this study ( $^{10}\text{Be}$  open circles,  $^{26}\text{Al}$  black circles) and from Chadwick et al., (1997) (open triangles). The site of the terrace sample is shown adjacent to paired  $^{10}\text{Be}$  and  $^{26}\text{Al}$  model ages. Our WR-3 age is the mean of the ages obtained from four separate sites (3A, 3B, 3D, and 3E), and agrees closely with the age measured by Chadwick et al., (1997). Mean rates of river incision between terrace levels inferred from our oldest terrace ages are shown along lines connecting terrace ages. The rates of incision from WR-7 to WR-3 deposition is based on the ash date of  $\sim 660$  ka for WR-7. Rates of incision increase through time in Chadwick et al. (1997) chronology; rates of incision decrease through time with our ages. Bottom graph shows oxygen isotope curve for last 700 ka (Imbrie et al., 1984) for comparison to terrace ages, with grayed boxes showing tentative correlations between terrace ages and the oxygen isotope curve.

to 137 ka) on WR-3 are similar to the  $^{36}\text{Cl}$  ages reported by Phillips et al. (1997) (Table 1) that were obtained from several large, flood-deposited boulders on WR-3 near Dinwoody Lakes, and suggested that the technique of inheritance correction works for this terrace. Estimated average rates of incision since WR-3 time range from  $0.21 \pm 0.05$  to  $0.59 \pm 0.13$  m/ka, decreasing downstream.

#### 4.3.2. Terraces WR-7, WR-9, and WR-15

We have also collected samples from terraces older than WR-3: the two extensive terraces WR-7

and WR-9, and the oldest terrace, WR-15. We have only surface samples from WR-7 sites 7A and 7B, which yield CRN model ages, not corrected for inheritance, of  $151 \pm 31$  ka and  $315 \pm 68$  ka using  $^{10}\text{Be}$ , and  $140 \pm 22$  ka and  $300 \pm 52$  ka using  $^{26}\text{Al}$ . The WR-9 site 9B profile using gravel and the WR-15 site 15A profile are exponential as would be expected (Eqs. (1) and (2), Fig. 7). Duplicate samples amalgamated from clasts collected at the same depth yield concentrations that agree well (Fig. 7), differing by typically  $< 20\%$ , suggesting mean inheritance is well constrained. Linear regression on

profiles from WR-9 site 9B cobbles yields model ages of  $204 \pm 24$  ka using  $^{10}\text{Be}$  and  $170 \pm 13$  ka using  $^{26}\text{Al}$ , WR-9 site 9B sands  $84 \pm 12$  ka using  $^{10}\text{Be}$  and  $112 \pm 9.0$  ka using  $^{26}\text{Al}$ , and from WR-15 site 15A  $509 \pm 37$  ka using  $^{10}\text{Be}$  and  $431 \pm 29$  ka using  $^{26}\text{Al}$  (Table 3; Fig. 8). WR-9 site 9A gives CRN ages that are quite old but with large errors (Table 3); we do not yet have a reasonable explanation for this, and we, therefore, neglect discussion of this anomaly. The errors on these ages are regression errors, and do not include rate of production or analytical errors. Except for the 9A site, all of these CRN model ages underpredict the previous age estimates for these terraces by  $\geq \sim 50\%$  (Table 1; Chadwick et al., 1997). Several possible reasons for this include: (1) the terrace surfaces have in the past been mantled by material (e.g., loess) that has since been stripped off, the most likely scenario; and (2) the new CRN ages are correct, and require revision of the old chronology.

We first consider the possibility that the terraces have been mantled, on average, by more loess since deposition than is currently present. If this is the case, the mean rates of production that the samples have experienced are lower than we would estimate on the basis of the current depth and lead to the low age estimates. The likelihood of eolian deflation and erosion of depositional surfaces through time in the Wind River basin is well-supported by studies on soil profiles (Chadwick et al., 1994; Dahms, 1994), although the history or magnitude of the erosion of the surface is not easily constrained. Assuming that the terrace ages of Chadwick et al. (1997) are correct based upon the dating of ash, we can quantitatively estimate the mean thickness of loess cover since terrace deposition needed to make the concentrations of CRN match those ages. Assuming the terrace deposits were covered by a silt with a  $z^*$  of  $\sim 100$  cm, the mean thicknesses of silt required are  $\sim 0.6$ – $0.8$  m for site 7A and  $\sim 1.1$ – $1.4$  m for site 7B to produce an age of  $\sim 660$  ka,  $\sim 1.3$  m for site 9B to match an age of  $\sim 940$  ka, and  $\sim 0.72$ – $0.99$  m for site 15A to match an age of  $\sim 1740$  ka. Given the present thicknesses of silt of  $\sim 30$ – $40$  cm on the terraces, terrace deflation is a reasonable explanation for the discrepancies between our ages and those of Chadwick et al. (1997). The CRN profiles provide a means of estimating the magnitude of past silt cover,

which would be difficult to constrain in any other way. As a cautionary note, an exponential CRN profile will be produced regardless of the history of the terrace surface above the samples; therefore, an exponential CRN profile cannot be used as evidence for a lack of surface change. Only the independent age control for the Wind River terraces, based primarily on the  $\sim 660$  ka ash date for WR-7, lead to the consideration of surface deflation as a possible complexity. The reliability of this ash date for WR-7 indicates terrace deflation may be the best interpretation for the wide discrepancy between our CRN ages and the existing chronology.

Another possible interpretation, although less plausible, is that our oldest CRN ages for WR-7 and WR-15 are correct, and previous age estimates need revision. Our WR-9 age is stratigraphically impossible given the ages for the other terraces; we, therefore, ignore it here. Several pieces of evidence may support revision, although none are conclusive. The existing terrace chronology of Chadwick et al. (1997) for terraces older than WR-3 relies entirely on two dates: (1) the CRN date for WR-3, and (2) the ash date for WR-7. These two ages imply an increase in the mean rates of incision in the Wind River from  $0.15$  m/ka between WR-7 and WR-3 to  $0.40$  m/ka from WR-3 to the present river. This acceleration would have to occur despite a  $\sim 20$ – $25\%$  decrease in the mean slope of the river during that time (Fig. 3). If instead we use the  $^{10}\text{Be}$  ages for sites 7A and 15A, the mean rate of incision at Bull Lake decreases from  $0.77$  m/ka between WR-15 and WR-7, to  $0.46$  m/ka between WR-7 and WR-3, to  $0.33$  m/ka WR-3 to WR-1, indicating a monotonic decrease in the rate of incision through time.

We also consider our ages relative to the glacial chronology. The model age of site 7A of  $\sim 300$  ka is consistent with CRN model ages of  $> 236$  ka (Evenson et al., 1994) and  $> 232$  ka (Phillips et al., 1997) obtained on moraines that appear to be stratigraphically correlated with the WR-7 terrace. If we assume that the terraces form during local glacial maxima coincident with periods of maximum volume of global ice, our terrace ages for site 7A and 15A can be roughly associated with global ice maxima in isotope stages 8 and 12 or 14, respectively (Fig. 8); assuming a constant rate of river incision between these two terraces, WR-9 may be associated



with isotope stage 10. This contrasts with the correlation of isotope stage where WR-7 is taken to be ~ 660 ka, which requires that the poorly preserved terraces WR-4 through WR-6 (Chadwick et al., 1997) record the fluvial response to glaciation between ~ 200 ka to ~ 600 ka. These correlations must be considered tenuous, because the uncertainties in these ages are large.

To accept this revision, we must reject the tephrochronology age for WR-7, and the other regional observations of rates of river incision accelerating toward the present (e.g., Reheis et al., 1991). Whereas the tephra has been well-dated, it may have been reworked from older terraces or deposits and incorporated into WR-7, making the tephra age a maximum for the terrace. The evidence for increasing rates of incision is harder to reconcile with our chronology, because even the Bighorn River, into which the Wind River flows, apparently follows this pattern (Palmquist, 1983). We, therefore, consider our ages for terraces WR-7 through WR-15 to be minima, given the likelihood of eolian erosion of the surfaces, the tephrochronology age, and the regional rate of incision increases through time. Our WR-3 ages appear reasonable, however, because they agree with independent dating efforts and are consistent for the four sample localities. Our work on the older terraces illustrates the continuing difficulty of precisely dating depositional surfaces older than a few 100 ka with CRN, because of the uncertainties in the geologic history of the surfaces and the large errors arising from calibrations of the rate of production, which are inherent in dating surfaces with CRNs. Although apparently reasonable ages may be ob-

tained from CRN profiles or surface samples, dating by other, independent methods and collection of CRN profiles from many sites on a surface are needed to check the validity of these ages.

#### 4.4. Cosmogenic inheritance

The estimated values for mean inheritance,  $\bar{N}_{in}$ , are given in Table 3 and are included on the CRN profiles (Fig. 7). The mean  $^{10}\text{Be}$  inheritance, between 7% and 20% of the total surface concentrations on WR-3 and WR-15 (Table 3), indicates that for terraces of this age and younger, inheritance is a significant source of CRNs. The mean inheritance in the terrace samples generally increases in the downstream direction (Table 3), perhaps reflecting increased average times of clast transport, or tributary contribution of clasts with greater mean inheritance. At the two sites where we collected sand and cobble samples (3B and 9B), the concentrations of CRN in the sand samples are lower than the cobble samples by ~ 30–50%, and imply that mean inheritance is lower for the sands; either exhumation or transport of sand through this fluvial system is substantially more rapid than cobbles. Quartz sands may provide a sample source with lower inheritance and a better constraint of the mean CRN given the large number of amalgamated grains.

We can use the proposed inheritance to estimate mean rates of erosion or transport times in this fluvial system (Anderson et al., 1996). Assuming all of the mean inherited concentration of CRN was produced during steady erosion from the clast source,

Table 4  
Erosion rates and time of fluvial transport estimated from CRN inheritance

Site	River km	CRN erosion rates (m/My)		CRN transport times (ky) <sup>b</sup>	
		$^{10}\text{Be}$	$^{26}\text{Al}$	$^{10}\text{Be}$	$^{26}\text{Al}$
3A	5	72	130	59	34
0A	57	34	42	130	110
3B (c)	57	31	50	140	90
3B (s) <sup>a</sup>	57	130	250	33	19
3C	73	69	44	62	100
15A	79	13	10	310	430
3E	89	18	23	230	190

<sup>a</sup>Note this is a sample amalgamated from quartz sand; all others from quartzite cobbles.

<sup>b</sup>Assuming mean burial depth of 5 m during transport.

the average rate of exhumation, for the amalgamated samples is:

$$\dot{\epsilon} = \frac{P_0 z^*}{\bar{N}_{in}} - \lambda z^* \quad (4)$$

The calculated mean rates of erosion are given in Table 4. Alternatively, we can assume all of the concentration of CRN, accumulated during the transport of the material from the source rock to the sample location. Ignoring decay, the mean concentration of a radionuclide accumulated during transport,  $N_{trans}$ , can be expressed:

$$N_{trans} = \bar{N}_{in} = P_0 T \left\{ \frac{1 - e^{-(H/z^*)}}{H/z^*} \right\} \quad (5)$$

where  $T$  is the mean total time in transit from source to deposit (including burial and transport) and  $H$  is the mean depth of the clast during transit, which we must estimate. In the Wind River system, the thickness of terrace gravels ranges from a few to  $\sim 25$  m (Chadwick et al., 1994); we have chosen an  $H = 5$  m for estimating the mean travel times given in Table 4. This choice for  $H$  is arbitrary, loosely constrained to lie between a minimum depth of 0 m (i.e., transport is accomplished only across the surface of the bed) and a maximum of  $\sim 25$  m, which is approximately the maximum depth of gravel measured on the terraces and in the modern river Wind River system.

The estimated mean rates of erosion range from 13 to 130 m/Ma (Table 4). These values are at the upper end to several times higher than previous CRN measurements of the rates of rock erosion in the Wind River Range ( $\sim 10$  m/Ma, Small et al., 1997) and elsewhere ( $\sim < 30$  m/Ma, Bierman, 1994). These measurements, however, were made on slowly eroding, bare-bedrock surfaces. On the other hand, our rates are quite similar to estimates of the mean rates of erosion obtained from sediment budgets in the basin (Ahnert, 1970). Assuming all of the arises during transport, the mean travel times generally increase in the downstream direction, and range from  $\sim 60$ – $310$  ka assuming a mean depth of transport of 5 m (Table 4). The estimated travel time is highly sensitive to the value chosen for  $H$  in Eq. (5), but even choosing  $H = 0$  m gives mean travel times exceeding a few thousand years, which suggests that

the clasts might remain in fluvial transport and storage for significant periods of time.

## 5. Conclusions

The multiple-sample, CRN profile technique is needed and apparently reliable for obtaining ages on depositional surfaces younger than  $\sim 150$  ka in the Wind River basin. The measured CRN inheritance represents a significant fraction of the total CRN abundance (up to  $\sim 20\%$  of surface concentrations), and is highly variable; inheritance must, therefore, be constrained to obtain reasonable model ages. Analysis of the modern river sample results indicates that amalgamation of many clasts ( $> 30$ ) are needed to obtain reasonable ( $< \pm 20\%$ ) estimates of the mean inheritance in this system. Our CRN profiles on the WR-3 terrace produce ages that are significantly corrected for inheritance, are consistent over four sample sites, agree with independent estimates of age, and highlight problems with the CRN histories of surface clasts. Based on the WR-3 results, we conclude that our CRN profile technique is a reliable method for dating with inheritance correction, despite the additional complexities introduced in sampling. Difficulty in dating the older terraces, however, emphasizes that considerable geologic caution, independent estimates of age, and multiple sample sites should ideally be part of dating depositional surfaces with CRNs.

Our model ages for the WR-3 terrace (mean of four sites =  $\sim 118$  to 125 ka) are consistent with a model of terrace formation during periods of maximum glacial extent, because they agree broadly with dates on Bull Lake-age moraines. The errors associated with the CRN technique, however, preclude further discrimination between formation during oxygen isotope stage 5 or 6 glacial advances. Our CRN ages for the older terraces (WR-7 =  $\sim 140$  to 300 ka and WR-15 =  $\sim 430$  to 510 ka) are very different from previous estimates, and require that either (1) significant changes in terrace silt cover have occurred since deposition of these terraces, or (2) that the previous chronology proposed for these surfaces is not correct. We believe the most plausible explanation for the discrepancy on terraces WR-7

through WR-15 is eolian deflation of these surfaces, which leads to prediction of ages that are too young. Silt caps with mean thicknesses of  $\sim 0.5$ – $1.5$  m since deposition are required to reconcile our concentrations of CRN with previous estimates of terrace ages. Mean thicknesses of silt through the terrace lifetime is a very difficult quantity to estimate by any other method, and is pertinent to studies of pedogenesis in such deposits. Acceptance of our CRN ages would require rejection of the tephrochronology age and the regional observation of increasing rates of river incision toward the present. We instead consider our age estimates on terraces WR-7 through WR-15 to be minima. The complications of geologic history, in addition to inherent CRN errors, suggest CRN dating of depositional surfaces requires that other, independent dating methods be used in conjunction with CRNs for surfaces older than  $\sim 150$  ka.

Measuring inheritance also allows rough estimation of maximum travel times in the fluvial system and minimum basin erosion rates. Assuming all inheritance comes from clast exhumation, we find minimum mean rates of exhumation of  $\sim 13$ – $130$  m/My for the quartzite source rocks in the Wind River Range. These rates are quite reasonable when compared to estimates of basin-wide rates of erosion determined using sediment budgets. Assuming instead that all inheritance comes from clast transport, we find the time of fluvial transport from source to terrace to be  $> \sim 10$  ka over several 10s to 100s of river kilometers, with an increase in the downstream direction and a decrease with decreasing grain size. Whereas the numbers obtained are not unique, the measurement of inheritance in clasts is a potentially useful tool for constraining clast exhumation and rates of transport; these rates are very difficult to obtain for long time scales by any other available methods.

### Acknowledgements

We appreciate the funding that has been provided to complete this work, which includes an IGPP-LLNL Center for Accelerator Mass Spectrometry grant, a Geological Society of America Cole Award, and an NSF—Presidential Young Investigator Award to

RSA, and a GSA Robert Fahnestock Fluvial Geomorphology grant and a UCSC Department of Earth Sciences grant to GSD. The manuscript was greatly improved through reviews provided by Dr. Peter Clark, Dr. Dennis Dahms, and an anonymous reviewer. We thank Gregory Pratt, James Repka, Dr. Justin Revenaugh, Daniel Sampson, and Eric Small for help with field and lab work, data analysis, and/or in reviewing drafts of this paper.

### References

- Ahnert, F., 1970. Functional relationships between denudation, relief, and uplift in large mid-latitude drainage basins. *American Journal of Science* 268 (3), 243–263.
- Anderson, R.S., Repka, J.L., Dick, G.S., 1996. Explicit treatment of inheritance in dating depositional surfaces using in situ  $^{10}\text{Be}$  and  $^{26}\text{Al}$ . *Geology* 24 (1), 47–51.
- Bierman, P.R., 1994. Using in situ produced cosmogenic isotopes to estimate rates of landscape evolution: a review from the geomorphic perspective. *Journal of Geophysical Research* 99 (B7), 13885–13896.
- Blackwelder, E., 1915. Cenozoic history of the mountains of central Wyoming. *Journal of Geology*, 23, pp. 97–117, 193–217, 307–340.
- Brown, E.T., Brook, E.J., Raisbeck, G.M., Yiou, F., Kurz, M.D., 1992. Effective attenuation lengths of cosmic rays producing  $^{10}\text{Be}$  and  $^{26}\text{Al}$  in quartz: implications for exposure age dating. *Geophysical Research Letters* 19 (4), 369–372.
- Cerling, T.E., Craig, H., 1994. Geomorphology and in-situ cosmogenic isotopes. *Annual Review of Earth and Planetary Sciences* 22, 273–317.
- Chadwick, O.A., Hall, R.D., Kelly, G., Amundson, R., Gosse, J., Phillips, F., Jaworowski, C., 1994. Quaternary Geology of the Wind River Basin, Wyoming (field trip guidebook). Friends of the Pleistocene, Rocky Mountain Cell.
- Chadwick, O.A., Hall, R.D., Phillips, F.M., 1997. Chronology of Pleistocene glacial advances in the Central Rocky Mountains. *Geological Society of America Bulletin* 109 (11), 1443–1452.
- Clark, D.H., Bierman, P.R., Larsen, P., 1995. Improving in situ cosmogenic chronometers. *Quaternary Research (New York)* 44 (3), 367–377.
- Dahms, D.E., 1994. Mid-Holocene erosion of soil catenas on moraines near the type Pinedale Till, Wind River Range, Wyoming. *Quaternary Research (New York)* 42 (1), 41–48.
- Elmore, D., Phillips, F., 1987. Accelerator mass spectrometry for measurement of long-lived radioisotopes. *Science* 236, 543–550.
- Evenson, E.B., Klein, J., Lawn, B., Middleton, R., 1994. Glacial chronology of the Wind River Mountains from measurements of cosmogenic radionuclides in boulders. *Geological Society of America Abstracts with Programs* 26, 511.
- Finkel, R.C., Suter, M., 1993. AMS in the Earth Sciences: technique and applications. *Advances in Analytical Chemistry* 1, 1–114.

- Forman, S.L., Smith, R.P., Hackett, W.R., Tullis, J.A., McDaniel, P.A., 1993. Timing of late Quaternary glaciations in the Western United States based on the age of loess on the eastern Snake River plain, Idaho. *Quaternary Research* (New York) 40 (1), 30–37.
- Gosse, J.C., Klein, J., Evenson, E.B., Lawn, B., Middleton, R., 1995. Beryllium-10 dating of the duration and retreat of the last Pinedale glacial sequence. *Science* 268 (5215), 1329–1333.
- Hall, R.D., Shroba, R.R., 1993. Soils developed in the glacial deposits of the type areas of the Pinedale and Bull Lake glaciations, Wind River Range, Wyoming, USA. *Arctic and Alpine Research* 25 (4), 368–373.
- Hall, R.D., Shroba, R.R., 1995. Soil evidence for a glaciation intermediate between the Bull Lake and Pinedale glaciations at Fremont Lake, Wind River Range, Wyoming, USA. *Arctic and Alpine Research* 27 (1), 89–98.
- Howard, A.D., 1970. A study of process and history in desert landforms near the Henry mountains, Utah. Doctoral thesis, The Johns Hopkins University.
- Imbrie, J.D., Hays, D.G., Martinson, D.G., McIntyre, A.C., Mix, A.C., Morley, J.J., Pisias, N.G., Prell, W.L., Shackleton, N.J., 1984. The orbital theory of Pleistocene climate: support from a revised chronology of the  $\delta^{18}O$  record. In: Berger, A., Imbrie, J., Hays, J., Kukla, G., Saltzman, B. (Eds.), *Milankovitch and Climate: Understanding the Response to Astronomical Forcing*, Part 1. Reidel, Bingham, MA, pp. 269–305.
- Jaworowski, C., 1992. A probable new Lava Creek ash locality: implications for Quaternary geologic studies in the western Wind River basin, Wyoming, USA. *Contributions to Geology, University of Wyoming* 29 (2), 111–117.
- Kohl, C.P., Nishiizumi, K., 1992. Chemical isolation of quartz for measurement of in-situ-produced cosmogenic nuclides. *Geochimica et Cosmochimica Acta* 56, 3583–3587.
- Lal, D., 1991. Cosmic ray labeling of erosion surfaces: in situ nuclide production rates and erosion models. *Earth and Planetary Science Letters* 104, 424–439.
- Love, J.D., 1979. Summary of Late Cenozoic history of the Wind River Basin and adjacent uplands in Wyoming. *US Geological Survey Professional Paper*, 1150, 75 pp.
- Morris, D.A., Hackett, O.M., Vanlier, K.E., Moulder, E.A., 1959. *Groundwater Resources of Riverton Irrigation Project*, Wyoming. *US Geological Survey Water-Supply Paper*, 1375, 205 pp.
- Nishiizumi, K., Winterer, E.L., Kohl, C.P., Klein, J., Middleton, R., Lal, D., Arnold, J.R., 1989. Cosmic ray production rates of  $^{10}Be$  and  $^{26}Al$  in quartz from glacially polished rocks. *Journal of Geophysical Research* 94 (B12), 17907–17915.
- Nishiizumi, K., Kohl, C.P., Arnold, J.R., Dorn, R.I., Klein, J., Fink, D., Middleton, R., Lal, D., 1993. Role of in situ cosmogenic nuclides  $^{10}Be$  and  $^{26}Al$  in the study of diverse geomorphic processes. *Earth Surface Processes and Landforms* 18, 407–425.
- Nishiizumi, K., Finkel, R.C., Klein, J., Kohl, C.P., 1996. Cosmogenic production of  $^7Be$  and  $^{10}Be$  in water targets. *Journal of Geophysical Research*, B, *Solid Earth and Planets* 101 (10), 22225–22232.
- Palmquist, R.C., 1983. Terrace chronologies in the Big Horn Basin, Wyoming. *Geological Association Guidebook for the 34th Annual Field Conference*, pp. 217–231.
- Patton, P.C., Biggar, N., Condit, C.D., Gillam, M.L., Love, D.W., Machette, M.N., Mayer, L., Morrison, R.B., Rosholt, J.N., 1991. Quaternary geology of the Colorado Plateau. In: Morrison, R.B. (Ed.), *Quaternary Nonglacial Geology: Conterminous U.S.* The Geological Society of America, Boulder, pp. 373–406.
- Phillips, F.M., Zreda, M.G., Smith, S.S., Elmore, D., Kubik, P.W., Sharma, P., 1990. Cosmogenic Chlorine-36 chronology for glacial deposits at Bloody Canyon, eastern Sierra Nevada. *Science* 248, 1529–1532.
- Phillips, F.M., Zreda, M.G., Gosse, J.C., Klein, J., Evenson, E.B., Hall, R.D., Chadwick, O.A., Sharma, P., 1997. Cosmogenic  $^{36}Cl$  and  $^{10}Be$  ages of Quaternary glacial and fluvial deposits of the Wind River Range, Wyoming. *Geological Society of America Bulletin* 109 (11), 1453–1463.
- Pierce, K.L., Obradovich, J.D., Freidman, I., 1976. Obsidian hydration dating and correlation of Bull Lake and Pinedale glaciations near West Yellowstone, Montana. *Geological Society of America Bulletin* 87, 703–710.
- Reheis, M.C., Palmquist, R.C., Agard, S.S., Jaworowski, C., Mears, B., Jr., Madole, R.F., Nelson, A.R., Osborn, G.D., 1991. Quaternary history of some southern and central Rocky Mountain basins; Bighorn Basin, Green Mountain–Sweetwater River area, Laramie Basin, Yampa River Basin, Northwestern Uinta Basin. In: Morrison, R.B. (Ed.), *Quaternary Nonglacial Geology: Conterminous U.S.* The Geological Society of America, Boulder, pp. 407–440.
- Repka, J.L., Anderson, R.S., Finkel, R.C., 1997. Cosmogenic dating of fluvial terraces, Fremont River, Utah. *Earth and Planetary Science Letters* 152, 59–73.
- Richmond, G.M., Fullerton, D.S., 1986. Summation of Quaternary glaciations in the United States of America. In: Sibrava, V., Bowen D.Q., Richmond, G.M. (Eds.), *Quaternary Glaciation of the Northern Hemisphere*. Pergamon, Oxford, pp. 183–196.
- Richmond, G.M., Murphy, J.F., 1965. *Geologic map of the Bull Lake East quadrangle, Fremont County, Wyoming*. GQ-431, U.S. Geological Survey Geologic Quadrangle Map.
- Ritter, D.F., 1967. Terrace development along the front of the Beartooth Mountains, southern Montana. *Geological Society of America Bulletin* 78, 467–484.
- Sinnock, S., 1981. Glacial moraines, terraces and pediments of Grand Valley, western Colorado. In: Epis, R.C., Callender, J.F. (Eds.), *Guidebook—New Mexico Geological Society: Western Slope, Colorado; western Colorado and eastern Utah*. New Mexico Geological Society, Socorro, NM, pp. 113–120.
- Small, E.E., Anderson, R.S., Repka, J.L., Finkel, R., 1997. Erosion rates of alpine bedrock summit surfaces deduced from in situ  $^{10}Be$  and  $^{26}Al$ . *Earth and Planetary Science Letters* 150 (3–4), 413–425.
- Talvitie, N.A., 1951. Determination of quartz in presence of silicates using phosphoric acid. *Analytical Chemistry* 23 (4), 623–626.
- Vincent, K.R., Chadwick, O.A., 1994. Synthesizing bulk density for soils with abundant rock fragments. *Soil Science Society of America Journal* 58 (2), 455–464.